Exploring low-energy nuclear properties: latest advances on reaction mechanisms with light nuclei

Brussels, 1-2 June 2023

Nuclear clusters for nuclear astrophysics studies

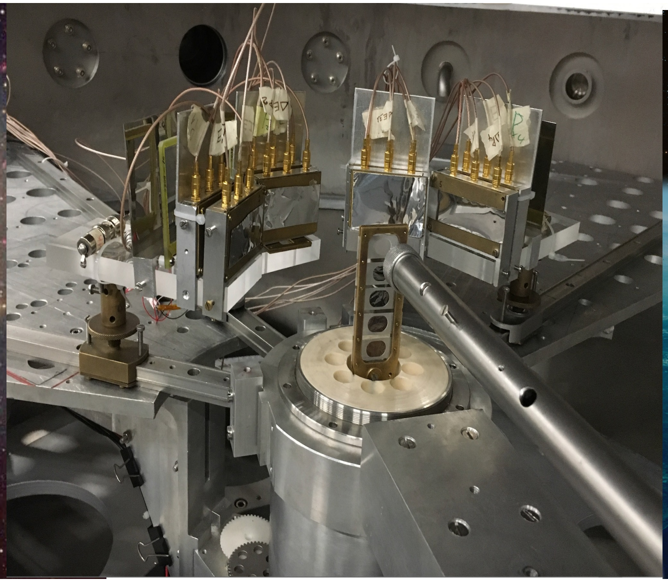

INFN Istituto Nazionale di Fisica Nucleare

Aurora Tumino

Outline

Clusters and their role in Nuclear Astrophysics

Indirect methods: focus on the THM

$^{12}C+^{12}C$ resonances and C-burning

The THM $^{12}C(^{12}C,\alpha)^{20}Ne$ and $^{12}C(^{12}C,p)^{23}Na$ experiment

Ikeda diagram

The threshold energies for each configuration are given in MeV. The smallest, unlabelled clusters are alpha particles. Increasing excitation energy is required to form evermore complex cluster structures.

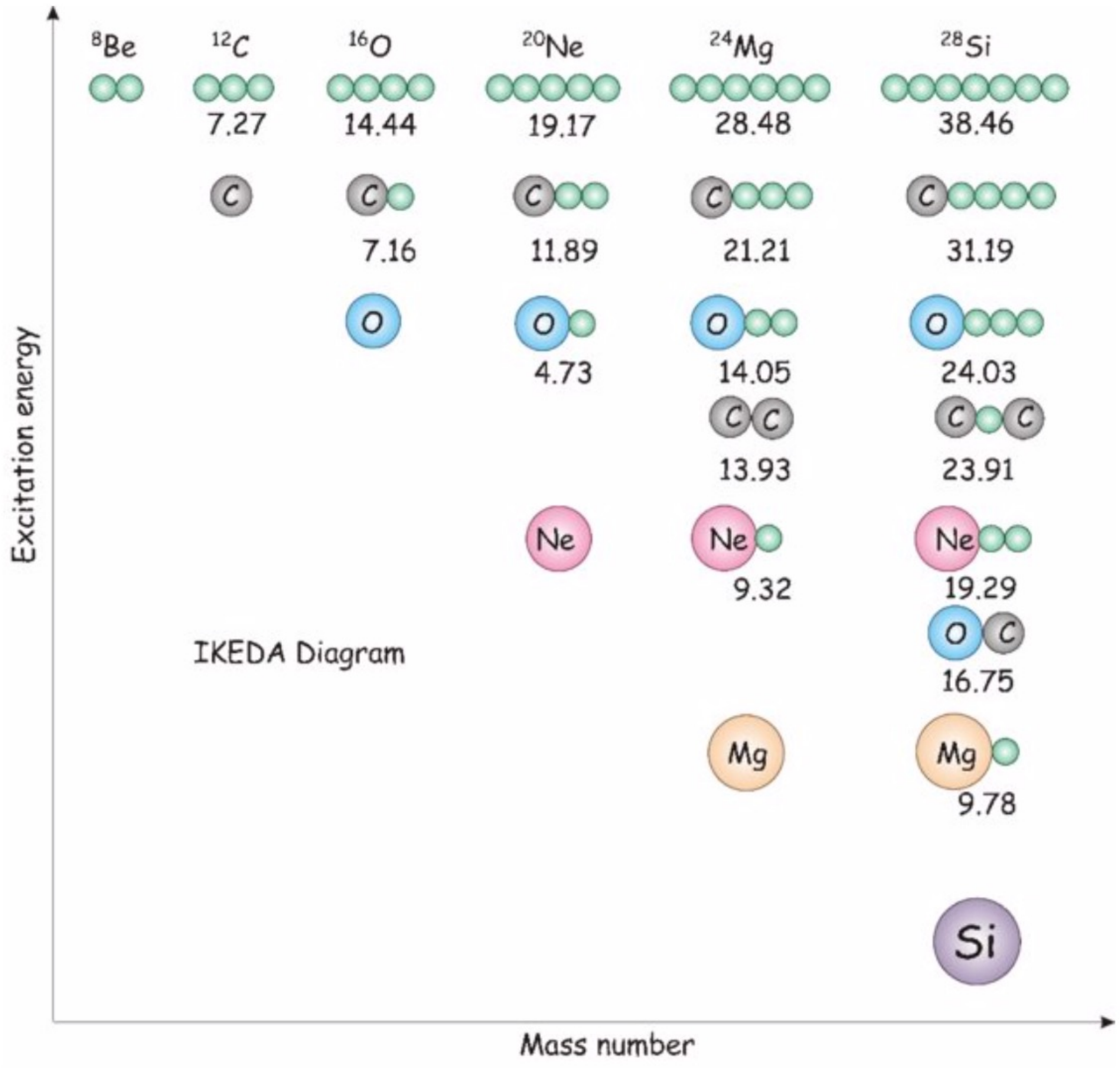

Nuclear clusters in He burning

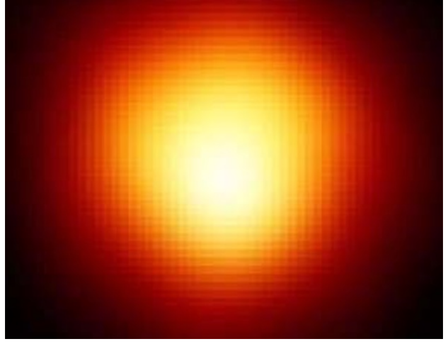

- 3α: $\alpha + \alpha \Leftrightarrow {}^{8}Be^{*} + \alpha \rightarrow {}^{12}C^{*} \rightarrow {}^{12}C$ (gs) Rate known to ± 10%

Hoyle state of ^{12}C located at 7.654 MeV (0^+), still a lot of discussion about the 3α configuration

- $^{12}C(\alpha,\gamma)^{16}O$ Poorly known (20-30%)

Gamow peak ~ 300 keV, where cross section enhancement is the result of interferences between resonances and nonresonant components, properties which are much more difficult to determine accurately.

The competition of these two reactions determines the $^{12}C/^{16}O$ ratio in our universe, and thus the late stellar evolution of massive stars and type Ia Supernovae.

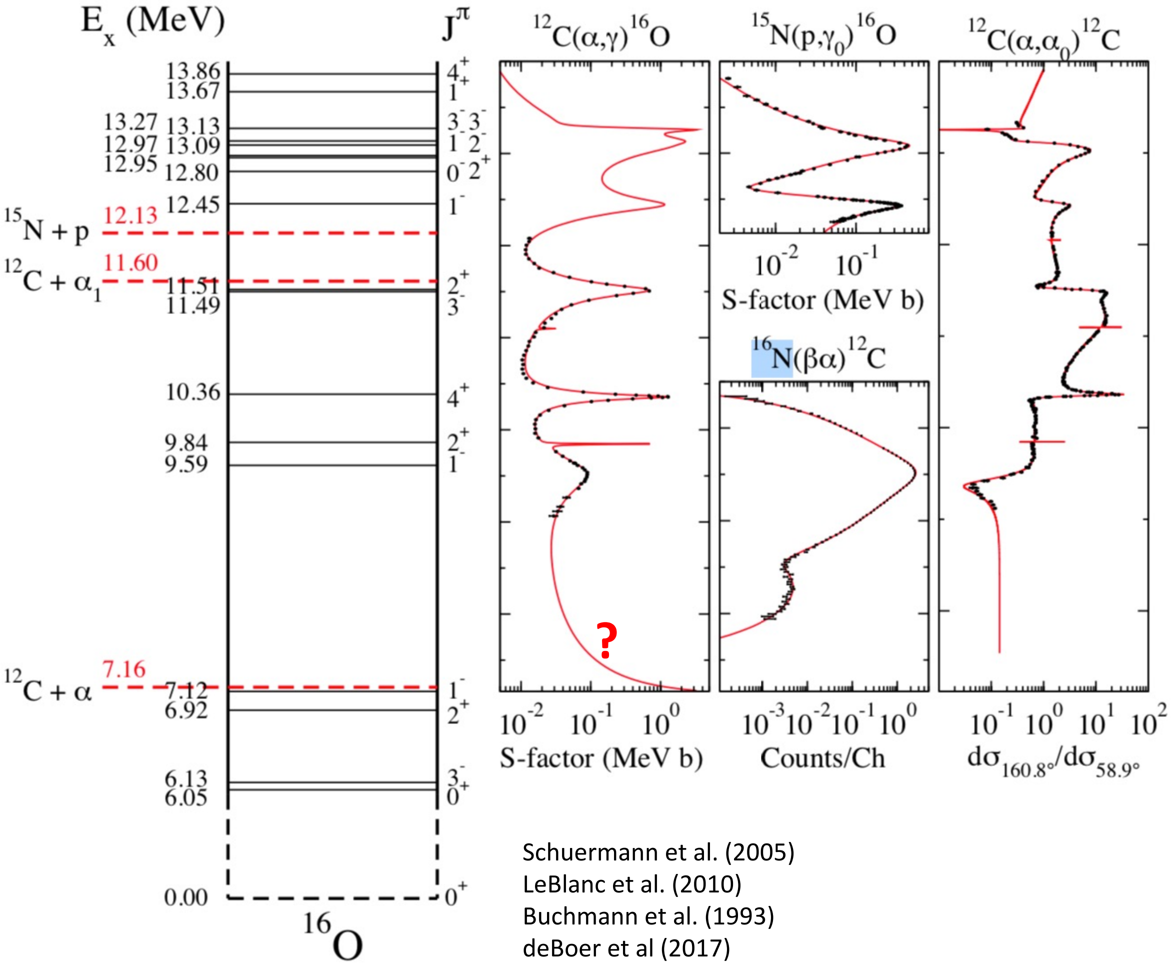

Schuermann et al. (2005)
LeBlanc et al. (2010)
Buchmann et al. (1993)
deBoer et al (2017)

Nuclear clusters in the nucleosynthesis of first stars

Enhanced carbon metals poor stars (CEMP): first stars formed about 100000 years after BBN, how to justify the observed pronounced enhancements of carbon, nitrogen, and oxygen abundances? Recent idea by Wiescher: nuclear clusters can push nucleosynthesis of CNO nuclei in the first stars bypassing the lack of A=5,8 stable nuclei.

2H(α, γ)6Li(α, γ)10B(α, d)12C
7Li(α, γ)11B(α, p)14C.

Clusters responsible for nuclear deformation and reduction of the Coulomb barrier, however in most of the cases we are still limited by the Coulomb barrier …

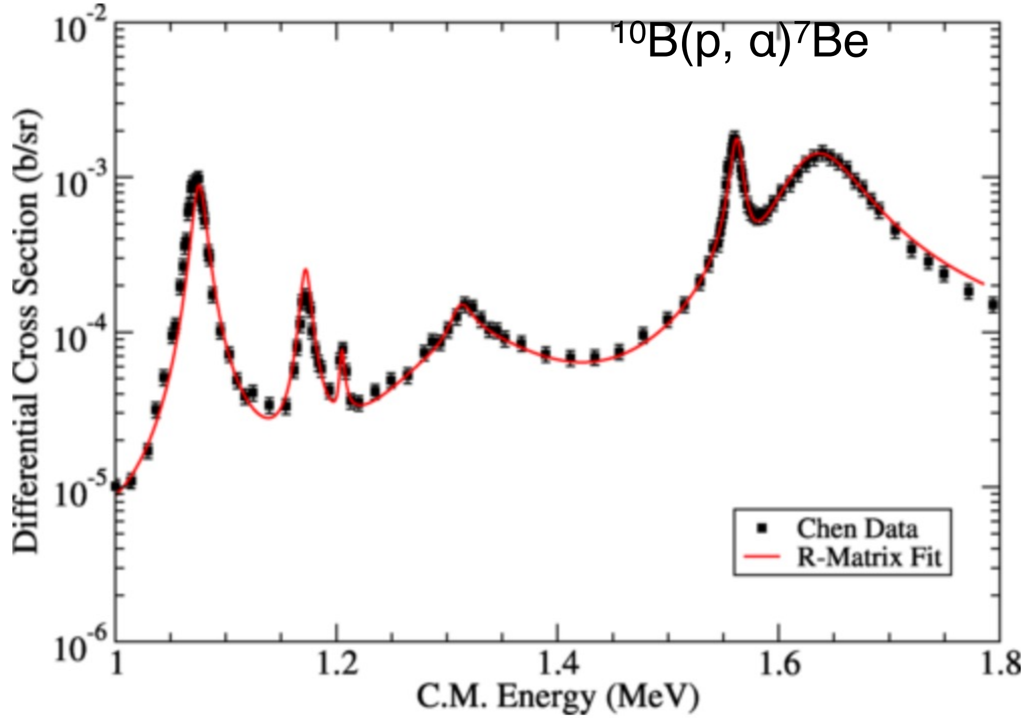

α-capture reactions are balanced by the proton induced $^6Li(p,\alpha)^3He$ [11] and the $^{10}B(p, \alpha)^7Be$ reactions

Need to measure at low energy some standard reactions

A. Gula et al., PRC **107**, 025805 (2023)

RESONANCES IN C^{12} ON CARBON REACTIONS

E. Almqvist, D. A. Bromley, and J. A. Kuehner
Atomic Energy of Canada Limited, Chalk River Laboratories, Chalk River, Ontario, Canada
(Received March 28, 1960)

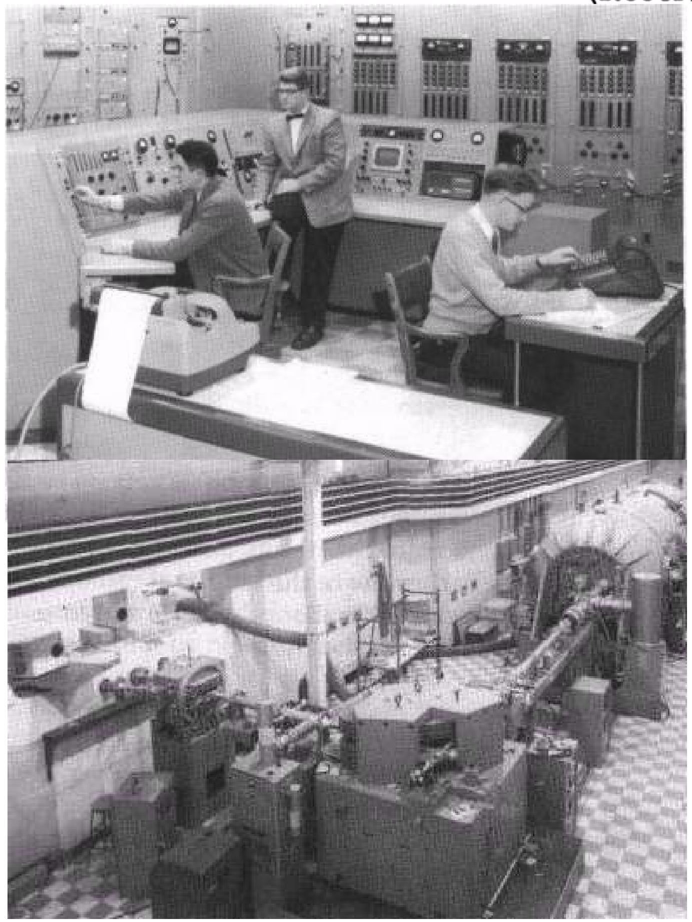

The world's first tandem accelerator
Installed at Chalk River in 1959

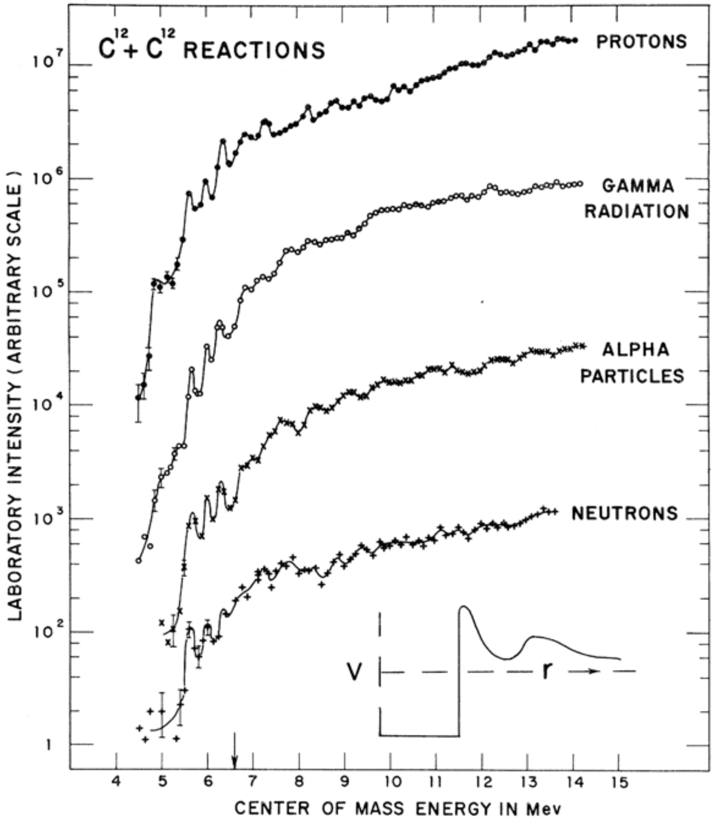

Molecular resonances in the $^{12}C+^{12}C$ fusion reaction

12C+12C rotational band

Phase shift analysis of 12C+ 12C elastic data from Ecm= 5 5 to 33 MeV has revealed a pronounced sequence of gross structure resonances. They appear to form a rotational band from l = 0 to at least 16h, and are the dominant structural feature of the 12C+12C reaction

Breit–Wigner resonance parameters used to fit fig. 1. The S-matrix elements S_l are parametrized as $S_l \equiv \eta_l \exp(2i\delta_l) = S_l^{bg}\{1 - i\exp(i\phi_l)\Gamma_l(^{12}C)/[(E - E_{res,l}) + i\frac{1}{2}\Gamma_{l,tot}]\}$, where S_l^{bg} was obtained from Woods–Saxon potential wells, $V_R = 60$ MeV, $r_R = 4.5$ fm, $a_R = 0.35$ fm, and $W = 40$ MeV, $r_I = 4$ 5 fm, $a_I = 0.35$ fm. A constant mixing phase $\phi_l = -15°$ was used for all l.

l	$E_{res,l}$ (MeV)	$\Gamma_l(^{12}C)$ (MeV)	$\Gamma_{l,tot}$ (MeV)	$\Gamma_l(^{12}C)/\Gamma_{l,tot}$
0	7.1	0 8	2.5	0.32
2	7.5	1.0	2.8	0 36
4	8.2	1.8	3.7	0.49
6	9.8	2.9	5.2	0.56
8	12.2	3.1	5.6	0.55
10	15.5	1.8	7.0	0.26
12	19.0	1 8	7.8	0.23
14	23.5	2.3	9.0	0.26
16	(28.0)	(2.0)	(10.0)	(0.20)

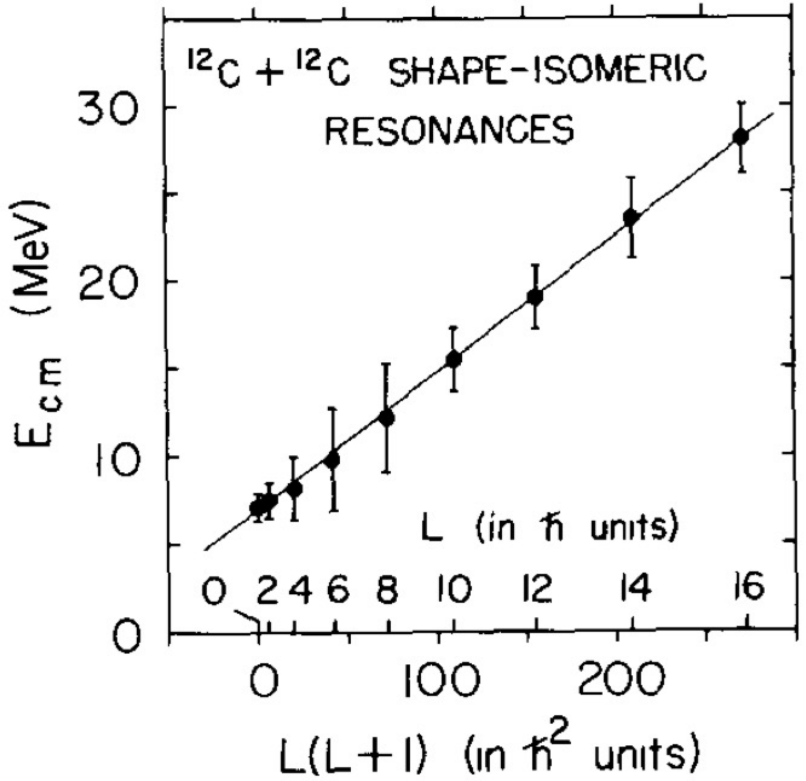

C.E. Ordonez et al., PLB 173, 39 (1986)

C-burning

-Carbon burning: third most important phase in the evolution and nucleosynthesis of massive stars ($> 8\ M_{\odot}$).

Starts like the sun:

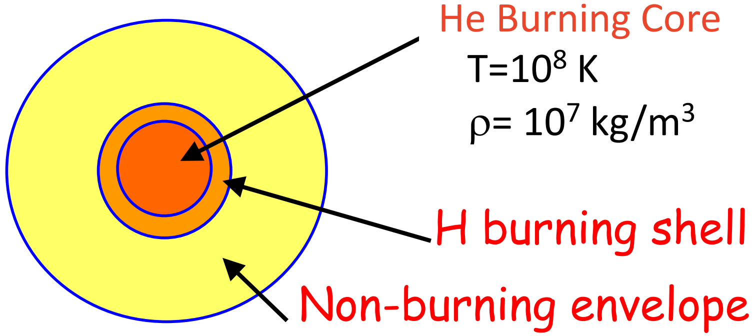

But now, when He is exhausted in the core and the core collapses, it does get hot enough to burn carbon and oxygen.

The successive stages in the core are H $\rightarrow$ He, gravity, He $\rightarrow$ C,O, gravity, $\rightarrow$ C,O $\rightarrow$ Mg, Si, gravity, Si $\rightarrow$Fe.

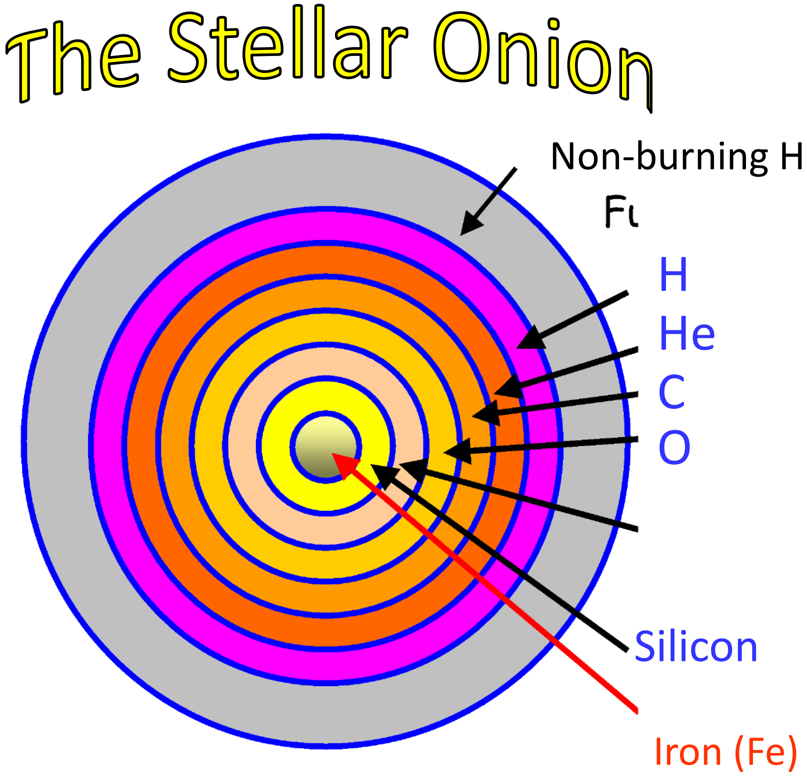

Carbon burning:
Relevant temperatures T ~ 0.6-1.2 GK and densities > 3 10^9 kg/m^3
More massive stars burn their nuclear fuel more quickly, since they have to offset greater gravitational forces to stay in (approximate) hydrostatic equilibrium. For example, a star of 25 solar masses burns hydrogen in the core for 10^7 years, helium for 10^6 years and carbon for only 10^3 years.

Carbon burning influences M_{up} minimum stellar mass required for hydrostatic carbon burning to occur. M_{up} is fundamental also for the evolution of supernova progenitors and white dwarf luminosity functions.

C-burning

- Engine for superbursts from accreting neutron stars

Relevant temperatures T ~ 0.4-0.7 GK

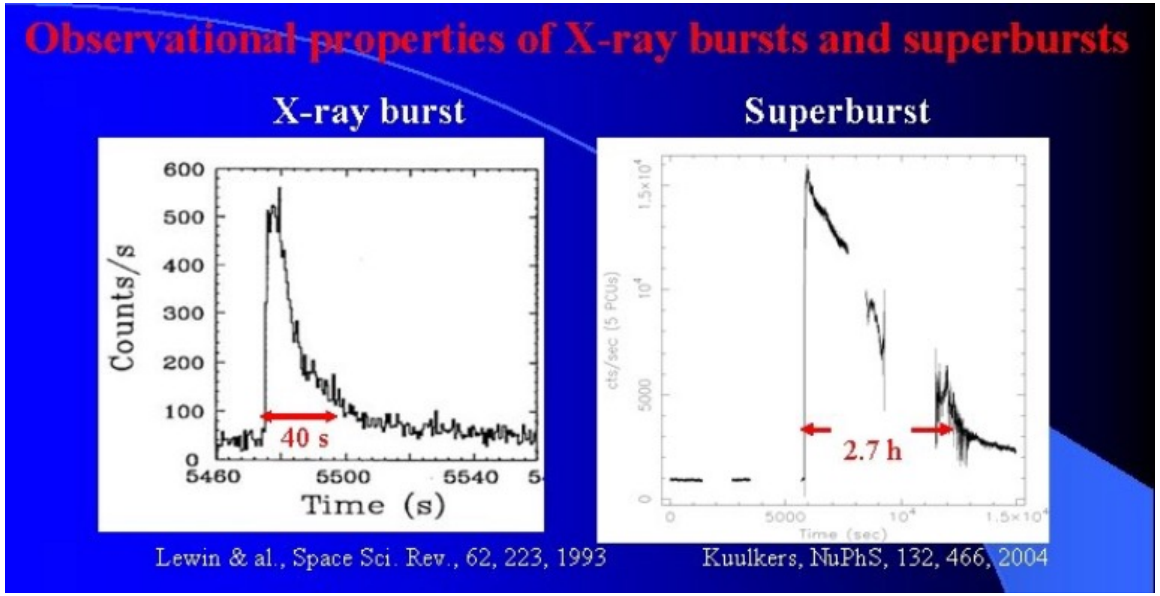

$L_{max} \cong 10^{38}$ ergs s^{-1}	$L_{max} \cong 10^{38}$ ergs s^{-1}
$E_{tot} \cong 10^{39}$ ergs	$E_{tot} \cong 10^{42}$ ergs
$t_{burst} \cong$ 10s – several min	$t_{burst} \cong$ several min – several hours
$t_{rec} \cong$ 5min - days	$t_{rec} \cong$ years

Source of superbursts: carbon burning in the outer crust?

Key problem: with the standard $^{12}C+^{12}C$ rate from CF88, the crust temperature is too low to ignite the carbon fuel → need to have resonances …

C-burning

- ignition conditions of Type Ia supernovae

They are thought to be thermonuclear explosions of white dwarfs (WD)
Their progenitors are not well understood, but their fates depend on the rate of $^{12}C+^{12}C$ reaction. Indeed, they are interpreted as the consequence of explosive carbon burning ignited near the core of the white dwarf star in a binary system

Relevant numbers: (0.15-0.7 GK and $\rho \sim (2-5)\ 10^9$ g/cm^3):
the C/O ratio influences the nucleosynthesis and, in turn, the resulting light curve

12C+12C fusion

Carbon burning mainly through $^{12}C+^{12}C$ fusion at E_{cm} from 1 to 3 MeV

Principal reactions:

$^{12}C(^{12}C,\alpha)^{20}Ne$	+ 4.617 MeV	The most frequent results of the interaction
$^{12}C(^{12}C,p)^{23}Na$	+ 2.241 MeV	
$^{12}C(^{12}C,n)^{23}Mg$	- 2.599 MeV	
$^{12}C(^{12}C,\gamma)^{24}Mg$	+13.933 MeV	
$^{12}C(^{12}C,2\alpha)^{16}O$	-0.20 MeV	

Considerable efforts to measure the $^{12}C+^{12}C$ cross section at astrophysical energies

M.G. Mazarakis & W.E. Stephensen, Phys. Rev. C 7 1280 (1973)
K. U. Kettner *et al.*, Phys. Rev. Lett. 38, 337 (1977)

H.W. Becker et al., Z. Phys. A 303, 305 (1981)
L. Barron-Palos et al., Nucl. Phys. A 779, 318 (2006)
E.F. Aguleira et al.,Phys. Rev. C 73, 064601 (2006)
T. Spillane et al., Phys. Rev. C 73, 064601 (2006)
T. Spillane et al., Phys. Rev. Lett. 98, 122501 (2007)
B. Bucher et al., Phys. Rev. Lett. 114, 251102 (2015)
C.L. Jiang et al., Phys. Rev. C 97 012801 (2018)
J. Zickefoose et al., Phys. Rev. C 97, 065806 (2018)
A. Tumino et al., Nature (2018)
G. Fruet et al. PRL, 124 192701 (2020)
W.P. Tan et al. PRL, 124 192702 (2020)

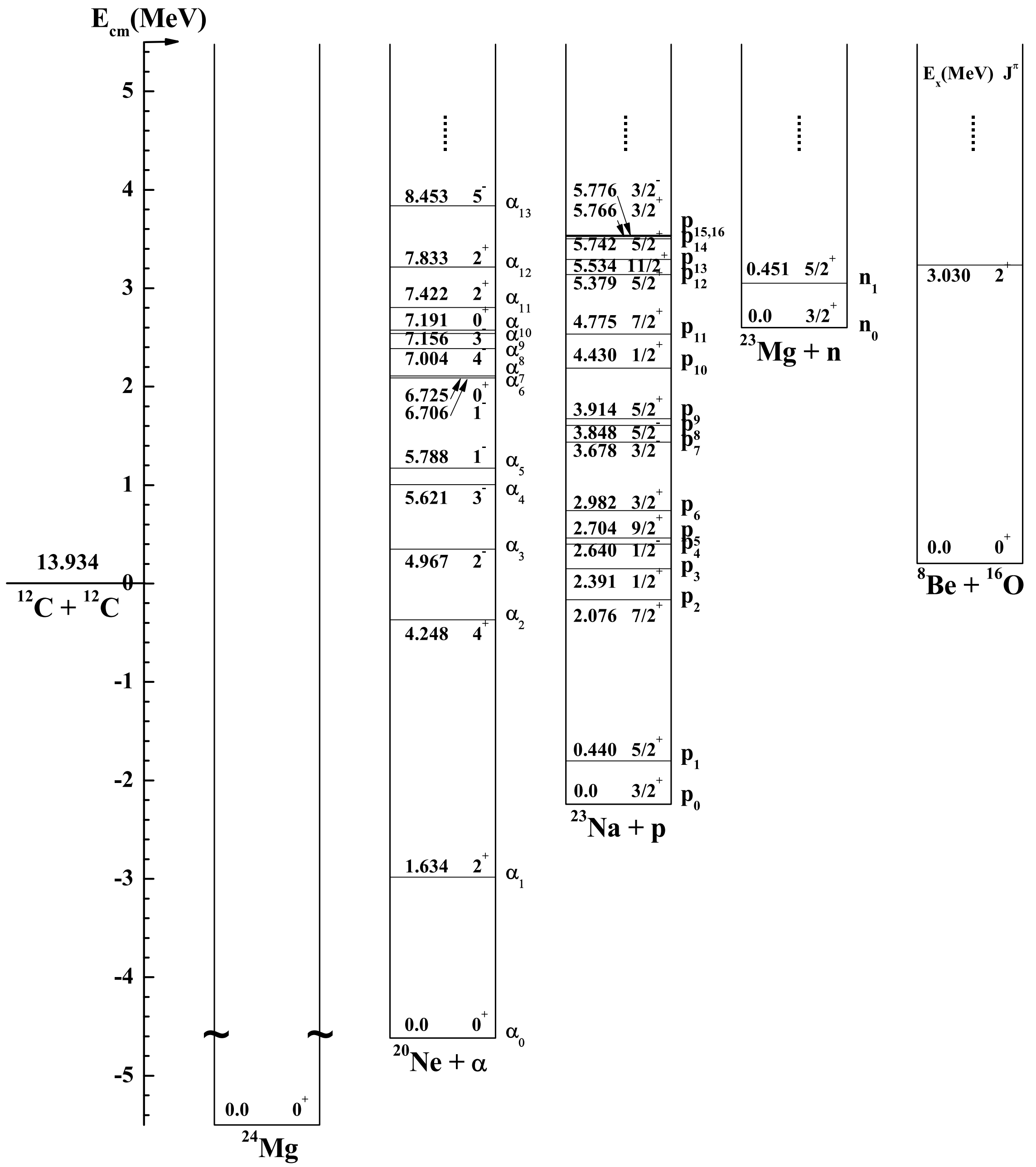

12C+12C: recent experiments

Jiang et al. 2018: down to $E_{c.m.}$ = 2.84 MeV and 2.96 MeV for the p and α channels, respectively, using a sphere array of 100 Compton-suppressed Ge detectors in coincidence with silicon detectors.

Fruet et al. 2020: down to $E_{c.m.}$=2.16 MeV using the particle-γ coincidence technique and thin C-target. Charged particles were detected using annular silicon strip detectors, while γ-ray detection was accomplished with an array of LaBr3(Ce) scintillators. Only the p_1 and α_1 channels. Total S* factor reconstructed taking not observed branchings from the literature

Tan et al. 2020: down to $E_{c.m.}$=2.2 MeV using the particle-γ coincidence technique and thick target. In particular, p and αs were detected using a silicon detector array, and γ-rays with HPGe detectors. Only the p_1 and α_1 channels. Total S* factor reconstructed taking not observed branchings from the literature.

Tumino et al. 2018: THM measurement down to 0.8 MeV for the $p_{0,1}$ and $\alpha_{0,1}$ channels. Coincidence experiment using the ^{14}N+^{12}C reaction at 30 MeV of beam energy.

All direct measurements: particle-γ concidence technique to further suppress the cosmic-ray background and some beam-induced background but no access to the ground state transitions

ground state transitions are crucial, as these channels contribute significantly at stellar energies

Charged particle cross section measurements at astrophysical energies

σ ~picobarn $\Rightarrow$ Low signal-to-noise ratio due to the Coulomb barrier between the interacting nuclei

measure $\sigma(E)$ over as wide a range as possible, then extrapolate down to E_0!

CROSS SECTION

$$\sigma(E) = \frac{1}{E} \exp(-2\pi\eta)\, S(E)$$

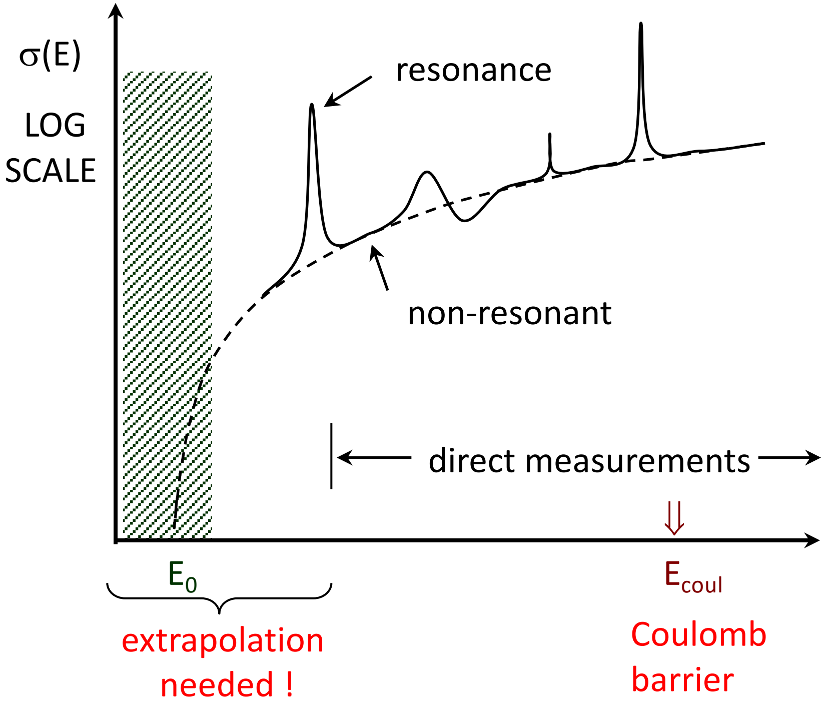

S-FACTOR

$$S(E) = E\sigma(E) \exp(2\pi\eta)$$

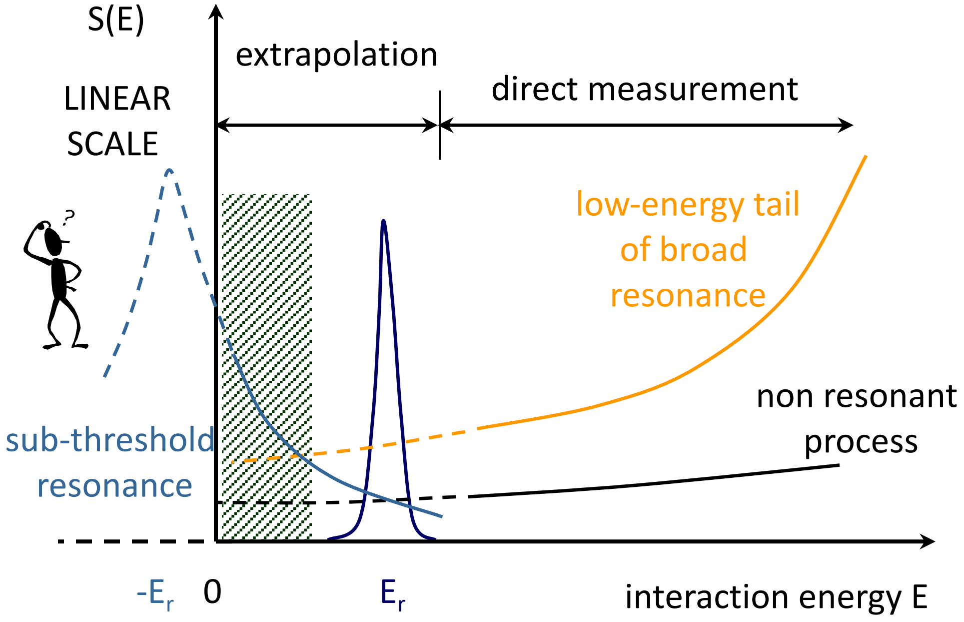

DANGER OF EXTRAPOLATION !

…but… intrinsic limitation at astrophysical energies → → → → Electron Screening

S(E) experimental enhancement due to the electron screening $S(E)_s = S(E)_b \exp(\pi\eta U_e/E)$

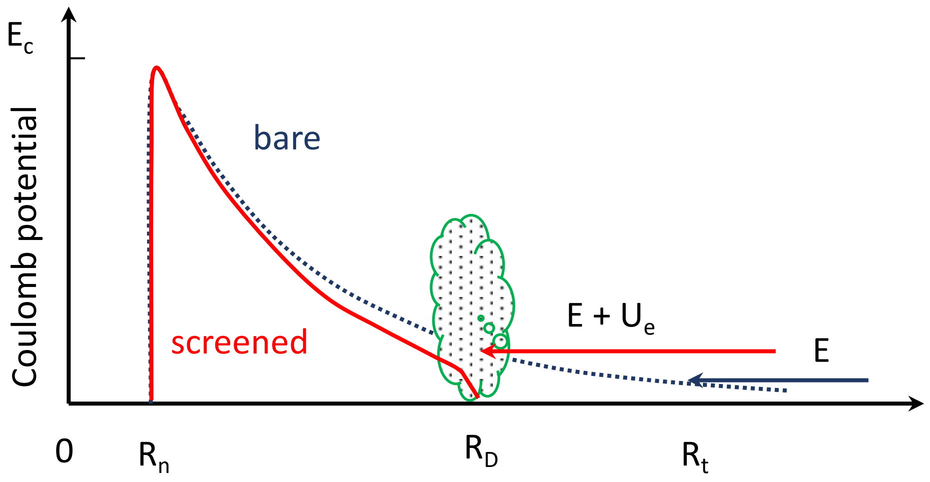

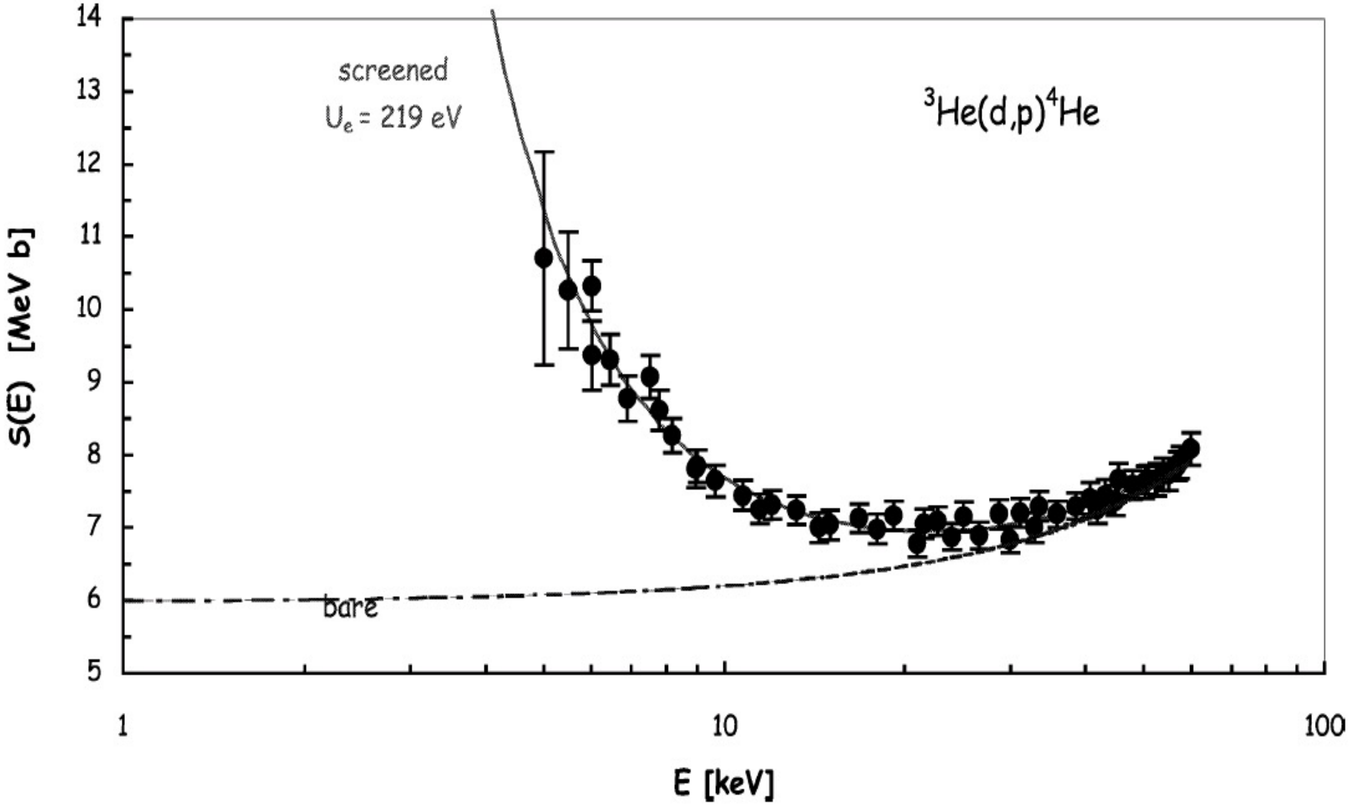

Electron Screening

In astrophysical plasma:

- the screening, due to free electrons in plasma, can be different

→ we need $S(E)_b$ to evaluate reaction rates

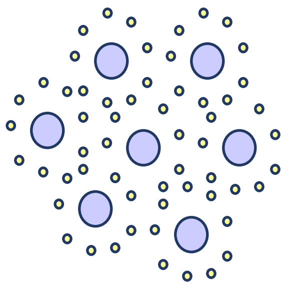

Debye-Hückel radius

$R_D \sim (kT/\rho)^{½}$

A theoretical approach to extract the electron screening potential U_e in the laboratory is needed

… however, experimental studies of reactions involving light nuclides have shown that the observed exponential enhancement of the cross section at low energies were in all cases significantly larger

(about a factor of 2)

than it could be accounted for from available atomic-physics model, i.e. the adiabatic limit $(U_e)_{ad}$ … screening yet to be fully understood

→ No way to measure $S(E)_b$ from direct experiments at energies where screening is important

$S_b(E)$-factor extracted from extrapolation of higher energy data

Indirect Methods for Nuclear Astrophysics

- to measure cross sections at never reached energies (no Coulomb suppression), where the signal is below current detection sensitivity
- to get independent information on U_e
- to overcome difficulties in producing the beam or the target (radioactive ions, neutrons..)

Quite straightforward experiment, no Coulomb suppression, no electron screening but …

Entrance channel

A+a → Several reaction mechanisms link the two channels → Reaction products

C+c+…

The reaction theory is needed to select only one reaction mechanism. However, nowadays powerful techniques and observables for careful data analysis and theoretical investigation.

Our Experiment with theTHM

$^{12}C(^{12}C,\alpha)^{20}Ne$ and **$^{12}C(^{12}C,p)^{23}Na$** reactions via the Trojan Horse Method applied to the **$^{12}C(^{14}N,\alpha^{20}Ne)^{2}H$** and **$^{12}C(^{14}N,p^{23}Na)^{2}H$** three-body processes

^{2}H from the ^{14}N as spectator s

Observation of ^{12}C cluster transfer in the $^{12}C(^{14}N,d)^{24}Mg^{*}$ reaction (R.H. Zurmûhle et al. PRC 49(1994) 5)

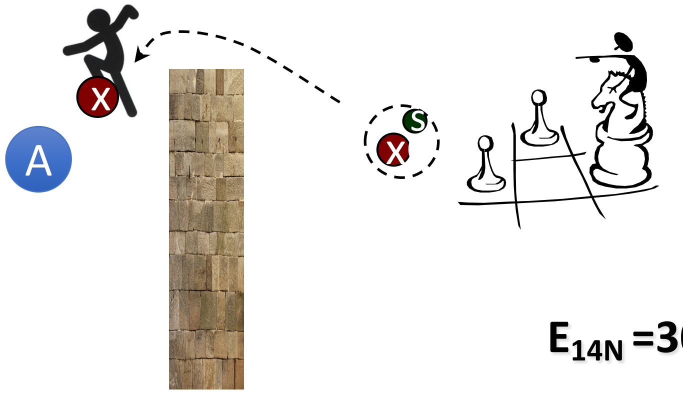

Repulsion wall

QUASI-FREE MECHANISM

✓ only ^{12}C - ^{12}C interaction

✓d = spectator

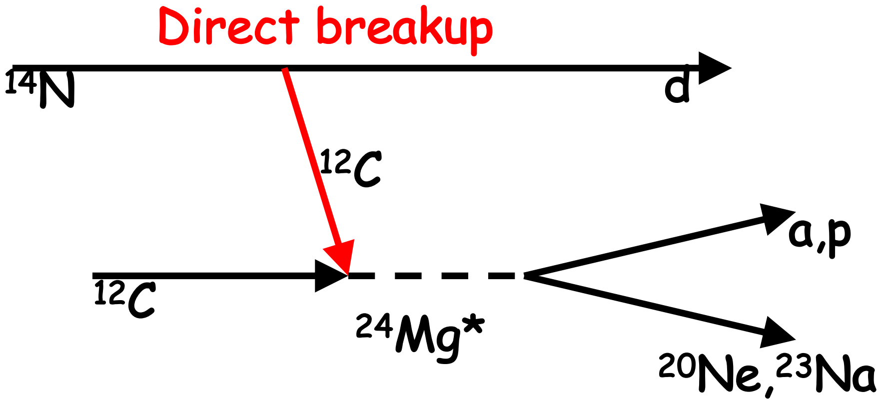

E_{14N} =30 MeV> E_{Coul}

⇒ **NO Coulomb barrier in the entrance channel**

NO electron screening

$$E_{QF} = E_{14N}\,\frac{m_{^{12}C}}{m_{^{14}N}}\cdot\frac{m_{^{12}C}}{m_{^{12}C}+m_{^{12}C}}\;-10.27\ \text{MeV}$$

PWIA approach to the THM

In the restricted phase space region where the quasi free kinematics holds true

$$\frac{d^3\sigma}{d\Omega_B d\Omega_b dE_B} \propto KF \left|\Phi(p_{xs})\right|^2 \left[\frac{d^2\sigma_{xA\to bB}}{dE_{xA}d\Omega}\right]^{HOES}$$

kinematical factor

momentum distribution of *s* inside *a*

Nuclear cross section for the A+x→C+c reaction

$$\frac{d^2\sigma_{xA\to c'}}{dE_{xA}d\Omega_s} = NF\sum_i (2J_i+1)\left|\sqrt{\frac{k_{c'}}{\mu_{c'}}}\frac{\sqrt{2P_{c'}}M_i(p_{xA}R_{xA})\gamma^i_{xA}\gamma^i_{c'}}{D_i(E_{xA})}\right|^2$$

From the modified R-matrix approach assuming non-interfering resonances

R-matrix fits on all channels at the same time in the full energy range of interest

$^{12}C+^{12}C\rightarrow\alpha_0+^{20}Ne$

$^{12}C+^{12}C\rightarrow\alpha_1+^{20}Ne^*$

$^{12}C+^{12}C\rightarrow p_0+^{23}Na$

$^{12}C+^{12}C\rightarrow p_1+^{23}Na^*$

Important: the same reduced widths appear in the THM and in the on-energy-shell cross-sections, so the ones extracted from THM data can be used to determine the direct *S*(*E*) factor, without HOES effects.

but No absolute value of the cross section → normalization to direct data available at higher energies

Selection of the quasi-free mechanism

Comparison between the experimental momentum distribution and the theoretical one

$$|\Phi(\overrightarrow{p_d})|^2 \propto \frac{\dfrac{d^3\sigma}{d\Omega_d d\Omega_{p,\alpha} dE_d}}{(KF)\left(\dfrac{d\sigma_{12C12C}}{d\Omega}\right)^N}$$

On-the-energy-shell bound state wave number ((see I.S. Shapiro, Soviet Physics Uspekhi Vol. 10, n. 4 (1968) and earlier works): $(2\mu_{d12C}B_{d12C})^{1/2}$=181 MeV/c.
Staying within this value is the condition for the QF mechanism to be dominant

Solid line: momentum distribution of d inside ^{14}N from the Wood-Saxon ^{12}C-d bound state potential with standard geometrical parameters r_0=1.25 fm, a=0.65 fm and V_0=54.427 MeV

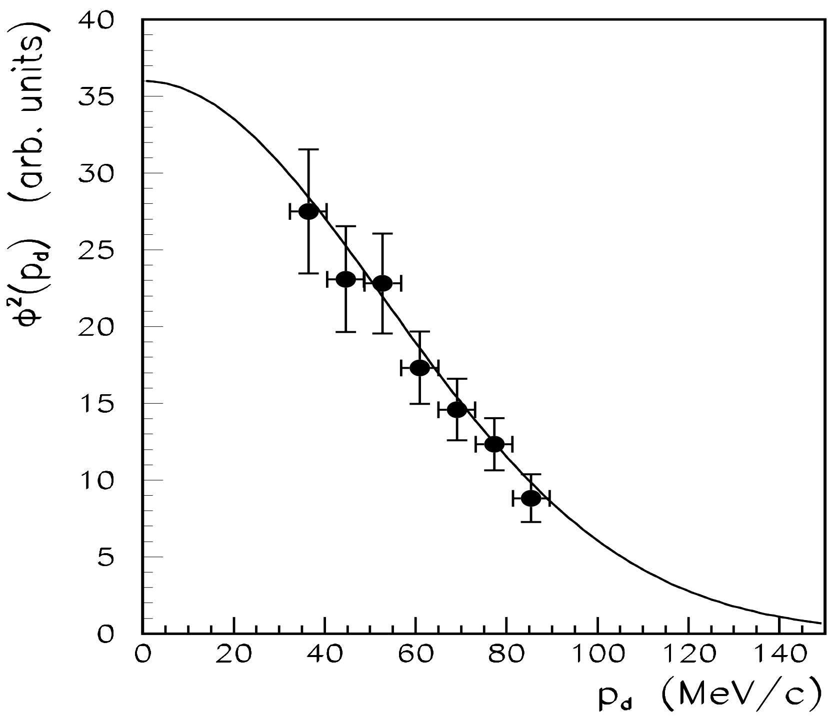

Plane Waves reliable also because:

- $p_d < (2\mu_{d12C}B_{d12C})^{1/2}$=181 MeV/c → Proved that the shape of the momentum distribution is insensitive to the theoretical framework used for its derivation (agreement between PWA and DWBA)

- the ^{14}N beam energy of 30 MeV corresponds to a quite high momentum transfer q_t=500 MeV/c giving an associate de Broglie wavelenght of 0.4 fm (< 3 fm=^{12}C+d)

Extraction of the two-body cross section

$$\frac{d\sigma_3}{dE} = KF|\varphi(p_s)|^2 \frac{d\sigma}{dE}$$

A. Tumino et al., Nature 557, 687 (2018)

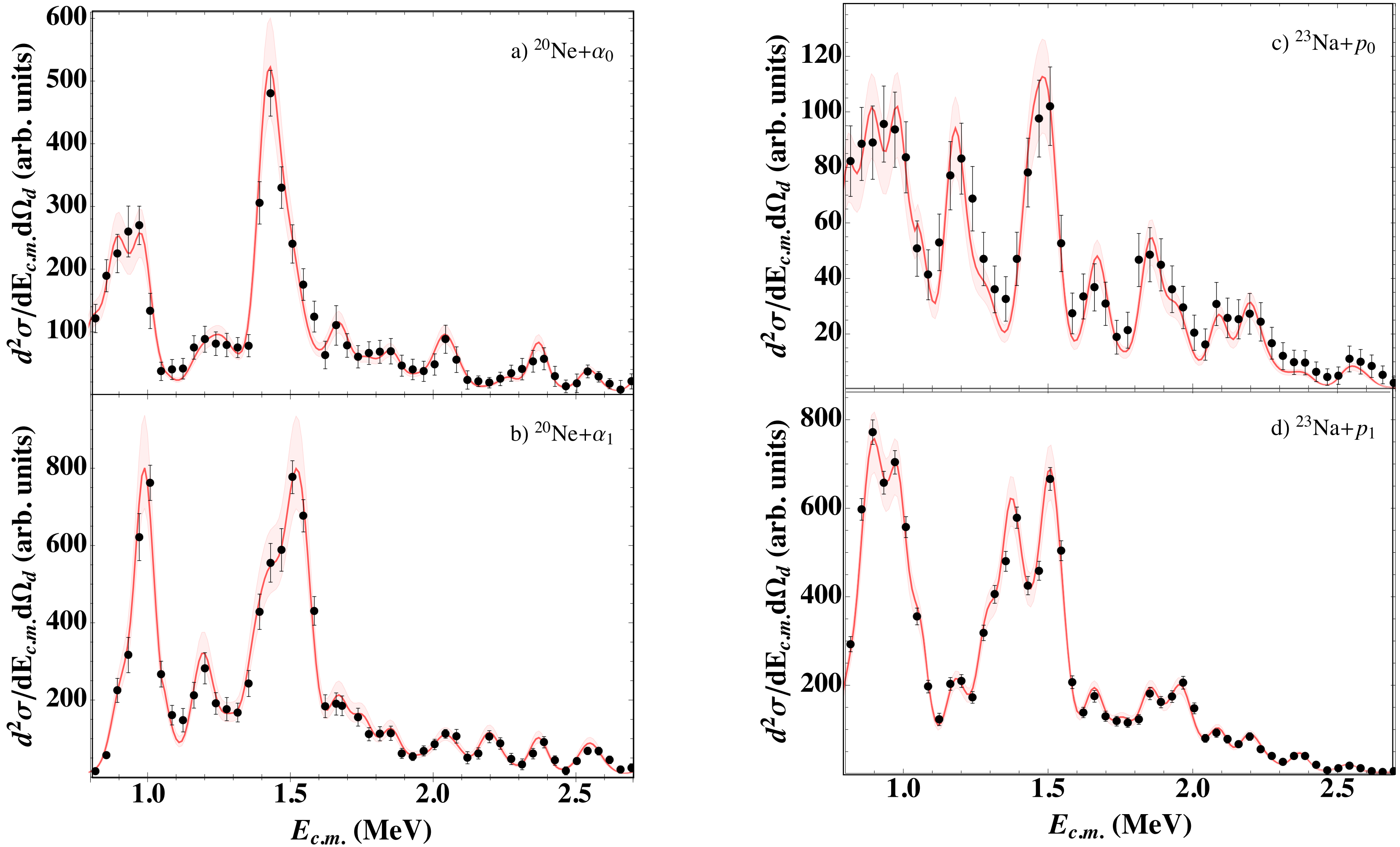

Red lines and bands: R-matrix fits for all channels at the same time

Reduced widths for known levels are used as free parameters to reproduce their total and partial widths as in Abegg & Davis, PRC 1991 → → →

12C+12C comprehensive figure

$^{12}C + ^{12}C \rightarrow \alpha + ^{20}Ne$

$^{12}C + ^{12}C \rightarrow p + ^{23}Na$

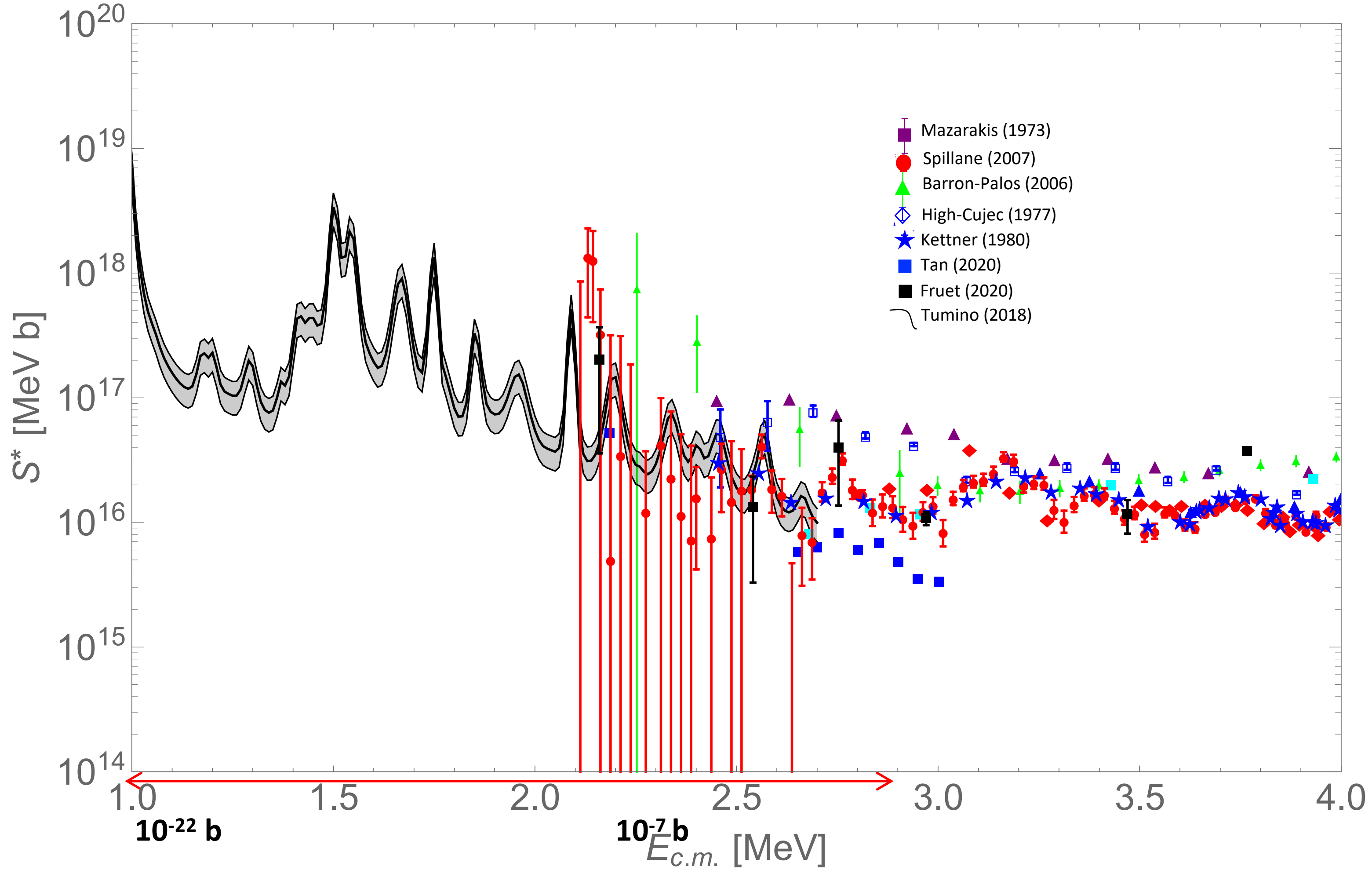

Next step:

- direct data below 2 MeV (LUNA MV, Notre Dame, Stella collaboration …)
- improve the normalization of THM data to direct ones with larger overlap

Nature volume 557, pages687–690 (2018) Published: 23 May 2018

LETTER

https://doi.org/10.1038/s41586-018-0149-4

An increase in the $^{12}C + ^{12}C$ fusion rate from resonances at astrophysical energies

A. Tumino[1,2]*, C. Spitaleri[2,3], M. La Cognata[2], S. Cherubini[2,3], G. L. Guardo[2,4], M. Gulino[1,2], S. Hayakawa[2,5], I. Indelicato[2], L. Lamia[2,3], H. Petrascu[4], R. G. Pizzone[2], S. M. R. Puglia[2], G. G. Rapisarda[2], S. Romano[2,3], M. L. Sergi[2], R. Spartá[2] & L. Trache[4]

12C+12C Reaction Rate

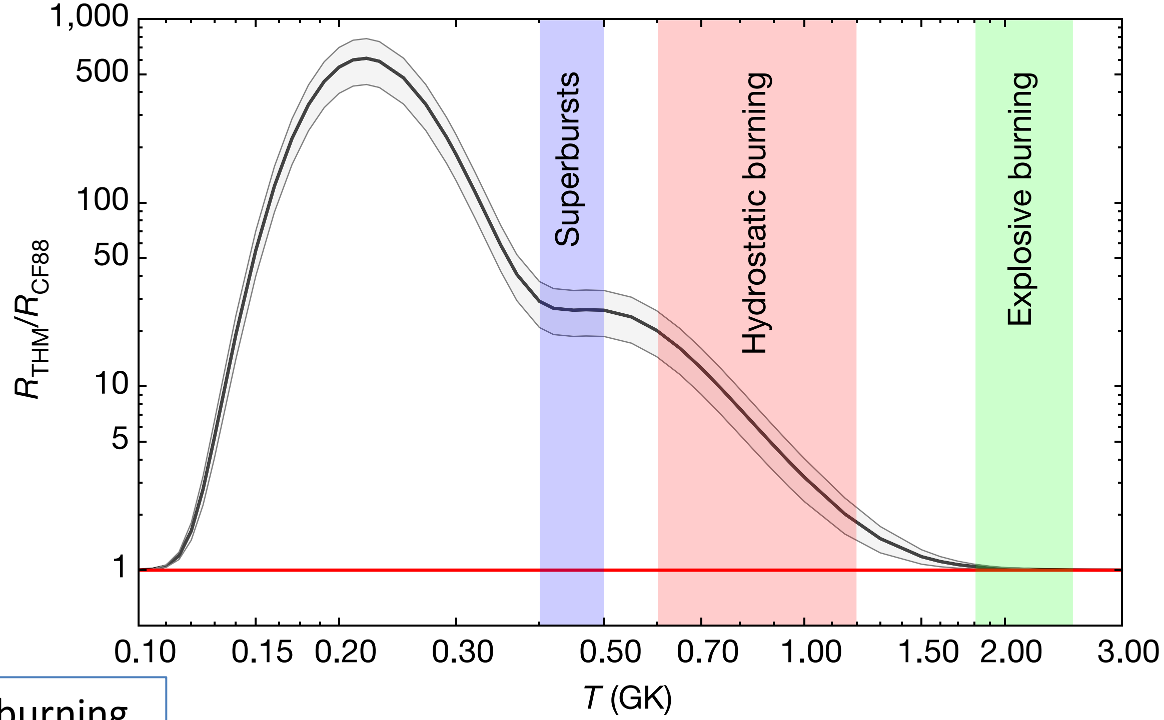

Color shadings mark typical regions for C-burning

Compared to CF88, the present rate increases from a factor of 1.18 at 1.2 GK to a factor of more than 25 at 0.5 GK

Some recent implications from the new 12C+12C rate

- Impacts of the New Carbon Fusion Cross Sections on Type Ia Supernovae (K. Mori et al. MNRAS 2018)

Partial solution of the Neutron star birthrate problem:

The NS birthrate has been estimated to be $10.8^{+7.0}_{-5.0}$ NSs/century, while the CCSN rate is estimated to be 1.9±1.1 SNe/century from measurements of γ-ray from ^{26}Al (Diehl et al. 2006; Keane & Kramer 2008), suggesting that the origin of NSs is supplemented by the so called Accretion Induced Collapse path of the WD mergers.

The enhanced reaction rate results in a lower ignition temperature, leading to a higher probability of finding WD-WD mergers reaching the Accretion Induced Collapse. This could increase the birthrate of the Galactic Neutron stars making the fraction of the WD mergers in the progenitors of type Ia SNe smaller.

To be continued … need to investigate the contribution of the DD scenario to SNe Ia, still largely subject to observational errors.

Some recent implications from the new 12C+12C rate

New investigation of the dependence of the compactness on the initial mass:

(A. Chieffi et al. ApJ 2021)

Compactness parameter ξ

(O' Connor & Ott 2011, ApJ 730,70)

$$\xi_i = \frac{M_i(M_\odot)}{R_i(10^3\ km)}$$

Best value → i=2.5 $M_\odot$

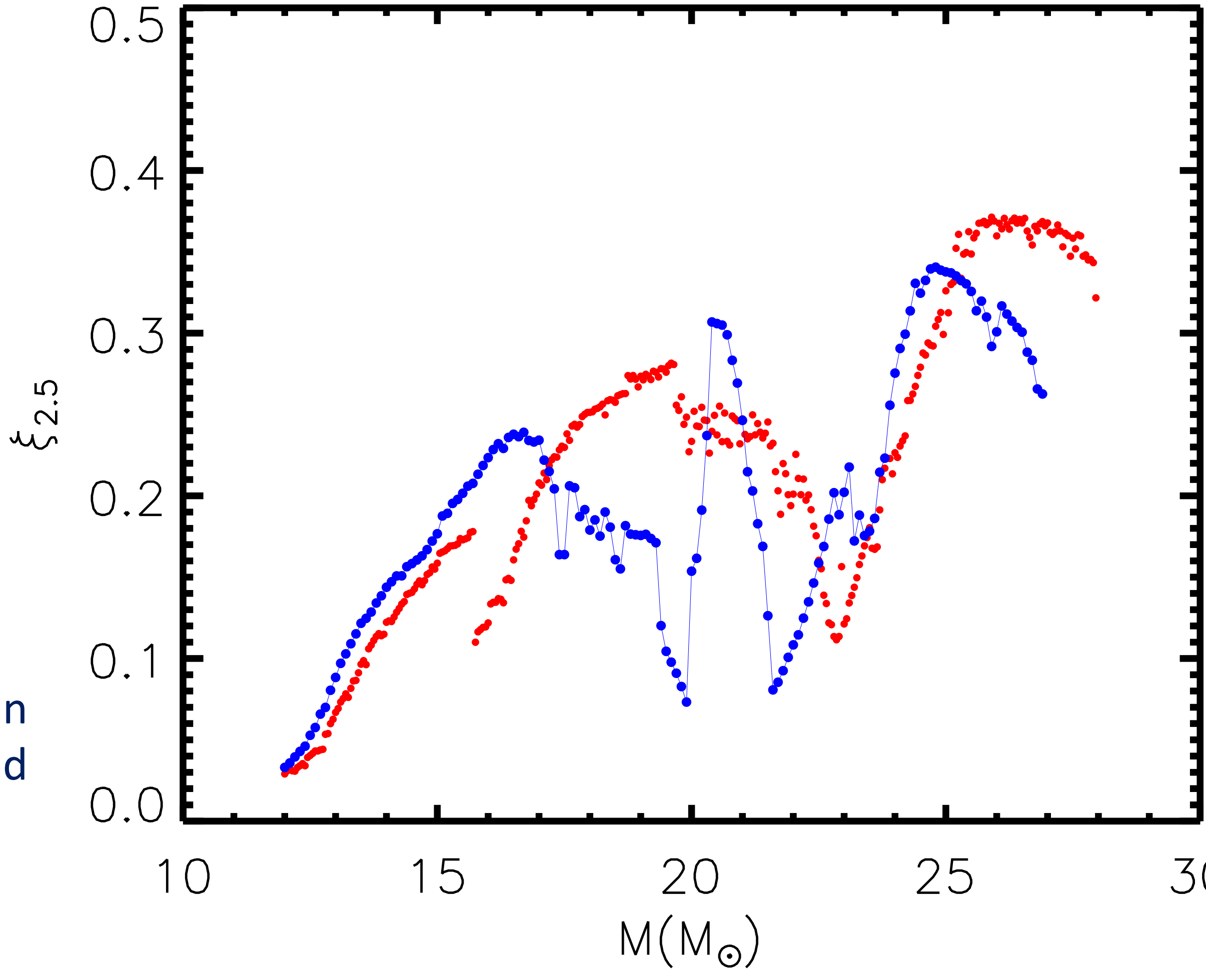

Scaling of the compactness of a star with the initial mass for two diffferent choices of the $^{12}C+^{12}C$ nuclear cross section:

red dots → CF88

blue dots →THM

It is quite evident that the adopted nuclear cross section plays an important role in determing the final compactness of a star and hence its final fate: explosion or collapse.

Remarkable lower compactness in some mass intervals, like between 17 and 20 $M_\odot$, and 21 and 23$M_\odot$, and above 25$M_\odot$. It would be interesting to follow with a 3D code what happens to the explosion …

Thank you!